

# Methylene Blue decolorization and Mineralization by Means of Electrochemical Technology at Pre-pilot Plant Scale: Role of the Electrode Material and Oxidants

Juliana Patrícia Souza Duarte Pontes, Patrícia Rachel Fernandes da Costa, Djalma Ribeiro da Silva, Sergi Garcia-Segura, Carlos Alberto Martínez-Huitle\*

Laboratório de Eletroquímica Ambiental e Aplicada (LEAA), Institute of Chemistry, Federal University of Rio Grande do Norte, Lagoa Nova, CEP 59078-970, Natal, RN, Brazil

\*E-mail: [carlosmh@quimica.ufrn.br](mailto:carlosmh@quimica.ufrn.br)

Received: 21 February 2016 / Accepted: 20 March 2016 / Published: 4 May 2016

---

In this work, a synthetic effluent containing methylene blue has been treated by electrochemical oxidation (EO) process at pre-pilot plant scale using a filter-press electrochemical cell reactor. Electrochemical experiments were carried out using Ti/Pt and Ti/IrO<sub>2</sub>-Ta<sub>2</sub>O<sub>5</sub> anodic materials in the presence or absence of chloride ions to study the influence on the decolorization and mineralization of the different oxidant species electrogenerated *in situ*. The electrochemical experiences have been carried out at different applied current densities ( $j = 20, 40$  and  $60 \text{ mA cm}^{-2}$ ) to evaluate the effect of this controlling parameter on the degradation efficiency and the operational energy consumption. Under optimal treatment conditions of  $40 \text{ mA cm}^{-2}$  in  $0.05 \text{ M}$  of Na<sub>2</sub>SO<sub>4</sub> at pH 6.0, solutions of  $100 \text{ mg L}^{-1}$  of methylene blue were completely decolorized obtaining 86.0 % of COD abatement after 360 min of electrolysis. The determination of energy consumption allowed to estimate operational costs about  $13.36 \text{ US\$ m}^{-3}$ . The results obtained provide valuable information regarding the EO process scaling-up, aiming the application of electrochemical technologies to treat actual effluent at real scale.

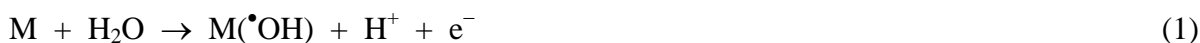
---

**Keywords:** dyes, dimensional stable anodes (DSA), wastewater treatment, anodic oxidation, electrochemical advanced oxidation processes (EAOPs),

## 1. INTRODUCTION

Electrochemical water treatment technologies are promising environmental friendly solutions to improve water quality for removing persistent hazardous pollutants. Among electrochemical technologies, the electrochemical advanced oxidant processes (EAOPs) demonstrate high efficiencies on the mineralization of highly persistent organic pollutants (POPs) by means of the electrogeneration

*in situ* of intermediary oxidant species such as reactive oxygen species or active chlorine species [1-4]. The simplest and most popular EAOPs is electrochemical oxidation (EO) where organic pollutants in solution are oxidized by direct charge transfer at the anode (M), or extensively destroyed by reactive oxygen species and/or active chlorine species electrogenerated by oxidation reactions onto the anode surface [1,2]. In the absence of chloride in solution, only reactive oxygen species are electrogenerated, such as hydroxyl ( $\bullet\text{OH}$ ) radical [1,5,6]. This oxidant species can react with most POPs up to complete combustion due to the high standard reduction potential ( $E^\circ(\bullet\text{OH}/\text{H}_2\text{O}) = 2.80 \text{ V/SHE}$ ) and its non-selective attack of organics. In EO the  $\bullet\text{OH}$  radical is produced as intermediate from water oxidation on anode materials with high over-potential of  $\text{O}_2$  evolution from reaction (1) [1,2], remaining adsorbed onto the anode surface.



where  $\text{M}(\bullet\text{OH})$  is the adsorbed hydroxyl radical onto the anode M that afterwards reacts with the pollutants in solution conducting to their mineralization or electrochemical combustion to  $\text{CO}_2$ .

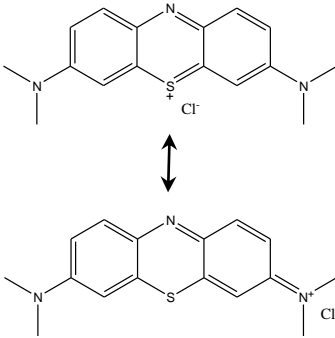
Meanwhile, in the presence of chloride, active chlorine species can be electrogenerated by  $\text{Cl}^-$  ion oxidation onto the anode releasing  $\text{Cl}_2$  from reaction (2) [4,7,8]. Afterwards, from the disproportionation of chlorine according reaction (3),  $\text{HClO}$  and  $\text{Cl}^-$  are released into the bulk. Due to the acid-base equilibrium (4) with  $\text{pK}_a = 7.55$ ,  $\text{ClO}^-$  could remain as predominant species in solution depending on the effluent pH. Besides,  $\text{ClO}^-$  could be directly yielded from chlorine reaction with  $\text{M}(\bullet\text{OH})$  according reaction (5) [4].



The quasi-ubiquitous presence of chloride ions in water effluents highlights the possible usage of EO technology [7] in order to promote the generation of active chlorine species by using particular electrocatalytic anodes, such as dimensional stable anodes (DSA). Also, the correct selection of DSA anode as well as suitable operating conditions avoid the production of chlorate and perchlorate ions [9,10].

Water pollution by dyestuff is a concerning environmental issue [11]. The dye release in water effluents produce water coloration that may reduce sunlight penetration and affect the photosynthetic activity of algae and the living beings of aquatic ecosystems [12,13]. Besides, several hazardous effects have been associated to these POPs such as suspicious carcinogenicity, mutagenicity and toxicity [11-15]. Methylene Blue (MB) is a cationic dye classified as basic dye according to the Color Index International. The main characteristics of MB are collected and summarized in Table 1. MB has been extensively used to dyeing paper, wool, silk and cotton [16]. Besides, it is well-known due to its application in cells/tissue staining and its prescription as antimalaric. However, an excessive exposure may precipitate serious serotonin toxicity, hypertension, dizziness and severe headache. MB can be found in some industrial effluents from dyeing process and manufacturing sites being its undesired side-effects as POP of high concern [16,17].

**Table 1.** Chemical structure and characteristics of Methylene Blue

Chemical Structure	Chemical formula	Chemical name	Common chemical name	Color Index name	Color Index number	$\lambda_{\text{max.}}$ /nm	M/g mol <sup>-1</sup>	Water solubility at 20 °C/g L <sup>-1</sup>
	C <sub>16</sub> H <sub>18</sub> ClN <sub>3</sub> S	3,7-bis(Dimethylamino)-phenothiazin-5-ium	Methylene Blue	Basic Blue 9	52015	664	319.85	40

The use of EO has shown promising results on the complete abatement of POPs in synthetic and real effluents such dyes [11,13,18], drugs [6,19-21], pesticides [22-24] and others [25-31]. However, these experiences have been commonly carried out at bench scale [2]. Hence, MB has been selected as model target pollutant to test the applicability of the designed flow filter-press cell electrochemical reactor. In this work we report the EO treatment of MB at pre-pilot plant scale by using both Ti/Pt and Ti/IrO<sub>2</sub>-Ta<sub>2</sub>O<sub>5</sub> anodes at different applied current densities. Moreover, the influence of the supporting electrolyte on the electrocatalytic behavior of the anodic materials has been assessed by means of the EO performance comparison in presence and absence of chloride ions in the treatment of solution.

## 2. EXPERIMENTAL

### 2.1 Chemicals

Commercial pure MB was purchased from Sigma-Aldrich. Anhydrous potassium sulfate and sodium chloride used as supporting electrolytes were of analytical grade supplied by Ventech. Solutions were prepared with high-purity water obtained from a Millipore Milli-Q system with resistivity >18 MΩ cm at 25 °C. All solutions were adjusted to pH 6.0 using either sulfuric acid and sodium hydroxide of analytical grade purchased from Sigma-Aldrich.

### 2.2. Electrolytic systems

An undivided filter-press electrochemical cell reactor was used to perform the EO treatment. The synthetic dye effluent was introduced into the 1 L reservoir and continuously recirculated through the electrochemical cell at 310 L h<sup>-1</sup> flow rate. The electrochemical filter-press cell schematized in Fig.1 presented an interelectrode gap of 1.3 cm between the electrodes of 63.5 cm<sup>2</sup> of geometric area.

Active anodic materials of Ti/Pt or Ti/IrO<sub>2</sub>-Ta<sub>2</sub>O<sub>5</sub> acquired from DeNora Electrodes (Italy) were used as anodes, whilst a Ti plate was used as cathode for all the electrolysis conducted. The experiences were carried out galvanostatically using a DC- MPL 3305M power supply at different applied current densities of 20, 40 and 60 mA cm<sup>-2</sup>.

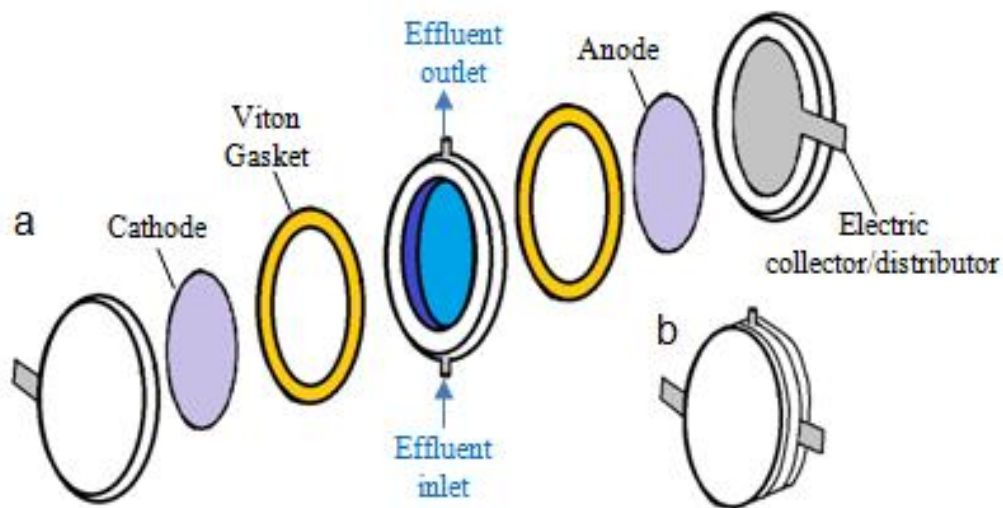


**Figure 1.** Electrochemical filter-press cell scheme (a) expanded cell and (b) attached operational cell.

Linear sweep voltammetry analyses were carried out using a potentiostat/galvanostat Autolab PGSTAT 302N controlled by NOVA 5.1 software. The experiences were carried out in a monocompartmental cylindrical electrochemical cell of 50 mL thermostated at 25 °C. The working electrodes were either Ti/Pt or Ti/IrO<sub>2</sub>-Ta<sub>2</sub>O<sub>5</sub> anodes, a Pt wire was employed as auxiliary electrode and all potentials were determined against an Ag/AgCl reference electrode with saturated KCl ( $E = 0.197$  V vs. SHE). The measurements were carried out at a scan rate of 50 mV s<sup>-1</sup> and under N<sub>2</sub> atmosphere after previous bubbling this gas through the solution for 10 min.

### 2.3. Apparatus and analytical procedures

The solution pH was measured and adjusted on a Tecnal pH-meter. Chemical oxygen demand (COD) concentrations were determined using the HANNA COD tube tests (range 0–1500 mg L<sup>-1</sup>) and a HANNA photometer COD-HI 83,099, after digestion procedure. From these values the percentage of COD abatement was estimated from expression (6) [26]:

$$\% \text{ COD} = \frac{\text{COD}_0 - \text{COD}_t}{\text{COD}_0} \times 100 \quad (6)$$

where COD<sub>0</sub> and COD<sub>t</sub> given in g O<sub>2</sub> dm<sup>-3</sup> are the initial chemical oxygen demands of the effluent and at the time t, respectively. From COD values the overall efficiency has been evaluated from the Instantaneous Current Efficiency (ICE, in.%) values for EO estimated from equation (7) [4]:

$$\% \text{ ICE} = FV \frac{(\text{COD}_0 - \text{COD}_t)}{8I\Delta t} \times 100 \quad (7)$$

where the applied current  $I$  (A),  $F$  the Faraday constant ( $96,487 \text{ C mol}^{-1}$ ),  $8$  is the oxygen equivalent mass ( $\text{g eq.}^{-1}$ ) and  $\Delta t$  is the electrolysis time in s.

The absorbance was determined at the maximum absorptivity of MB ( $\lambda_{\text{max.}} = 664 \text{ nm}$ ) using an UV-vis spectrophotometer Analytikjena SPECORD 210 PLUS, being the percentage of color removal of the solution estimated from equation (8) [12,13]:

$$\% \text{ Color Removal} = \frac{A_0 - A_t}{A_0} \times 100 \quad (8)$$

where  $A_0$  is the initial absorbance and  $A_t$  the absorbance at the treatment time  $t$ .

### 3. RESULTS AND DISCUSSION

#### 3.1. Electrochemical measurements

Preliminary experiments have been carried out by polarization curves to obtain information on the electroactivity of supporting electrolyte at electrodes, like Ti/Pt and Ti/IrO<sub>2</sub>-Ta<sub>2</sub>O<sub>5</sub>, prior to anodic oxygen evolution. Fig. 2 shows linear polarization curves of a Ti/Pt and Ti/IrO<sub>2</sub>-Ta<sub>2</sub>O<sub>5</sub> electrodes obtained in absence ( $0.05 \text{ mol L}^{-1}$  of Na<sub>2</sub>SO<sub>4</sub>) or in presence of chloride ( $0.02 \text{ mol L}^{-1}$  Na<sub>2</sub>SO<sub>4</sub> and  $0.017 \text{ mol L}^{-1}$  of NaCl) in solution with a scan rate of  $50 \text{ mV s}^{-1}$ . The curves are very different and show that oxygen evolution potential increases from  $1.44 \text{ V}$  to  $1.71 \text{ V}$  versus SHE for Ti/IrO<sub>2</sub>-Ta<sub>2</sub>O<sub>5</sub> and Ti/Pt [1,31,32], respectively. This means that Ti/IrO<sub>2</sub>-Ta<sub>2</sub>O<sub>5</sub> has low oxygen evolution overpotential and consequently is good electrocatalysts for the oxygen evolution reaction, while that Ti/Pt, even when potential is not very positive as showed by non-active electrodes, such as diamond films [2,4], it has high oxygen evolution overpotential than Ti/IrO<sub>2</sub>-Ta<sub>2</sub>O<sub>5</sub>, and consequently, it is a partial poor electrocatalyst for the oxygen evolution reaction. Later conditions indicate that, Ti/Pt anode promotes the production of hydroxyl radicals. Another important feature that can be indicated is that, Ti/Pt can promote the electrogeneration of other oxidant species from sulfate oxidation such as persulfate [2,33,34] following reaction (9), that could contribute to the decolorization of MB:



The results obtained in the presence of chloride ions, at both anode materials, are also shown in Fig. 2. In the case of the Pt/Ti anode, polarization curve is shifted to less positive potentials at the chloride concentration used (Fig. 2a). This behavior is mainly due to the increase of the importance of the reaction of Cl<sub>2</sub> evolution [2,4,27,34] and decreasing consequently its decolorization efficiency when it is used for electrochemical treatment [26]. Conversely, polarization curve is shifted to more positive potentials (Fig. 2b) at Ti/IrO<sub>2</sub>-Ta<sub>2</sub>O<sub>5</sub>, favoring the coexistence of reactive hydroxyl radicals, adsorbed at the anode surface and/or confined in a reaction cage around the electrode itself, as well as the oxychloro-radicals, often assumed as intermediates also in the chlorine evolution reaction. Mixture of oxidant species can further ease the electrochemical mineralization processes.

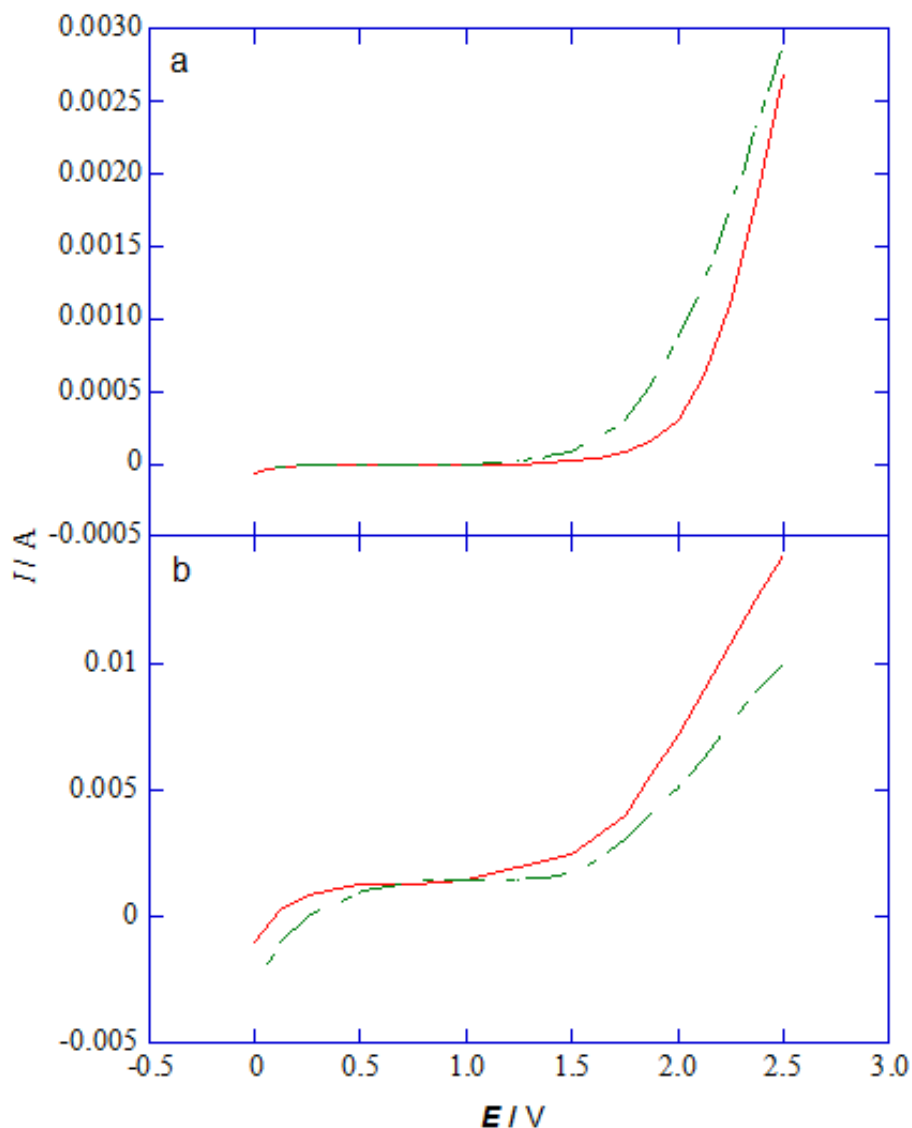


**Figure 2.** Polarization curves of (a) Ti/Pt and (b) Ti/IrO<sub>2</sub>-Ta<sub>2</sub>O<sub>5</sub> anodes as working electrodes at pH 6.0 and 25 °C with different supporting electrolytes: (●) 0.05 mol L<sup>-1</sup> of Na<sub>2</sub>SO<sub>4</sub> or (■) 0.02 mol L<sup>-1</sup> Na<sub>2</sub>SO<sub>4</sub> and 0.017 mol L<sup>-1</sup> of NaCl.

### 3.2. Supporting electrolyte effect on decolorization kinetics as a function of the anodic material

Figure 3 depicts the decolorization removal as a function of the electrocatalytic material (Ti/Pt or Ti/IrO<sub>2</sub>-Ta<sub>2</sub>O<sub>5</sub>) and supporting electrolyte (0.05 mol L<sup>-1</sup> of Na<sub>2</sub>SO<sub>4</sub> or 0.02 mol L<sup>-1</sup> of Na<sub>2</sub>SO<sub>4</sub> with 0.017 mol L<sup>-1</sup> of NaCl) used to treat solutions of 100 mg L<sup>-1</sup> of MB at pH 6.0 by means of EO at 60 mA cm<sup>-2</sup> during 360 min. When the MB solution is treated with Ti/Pt anode using solely Na<sub>2</sub>SO<sub>4</sub> as supporting electrolyte, higher decolorization performances were achieved (98%) in comparison with Ti/IrO<sub>2</sub>-Ta<sub>2</sub>O<sub>5</sub> which only reached 18.6 % of color removal after 360 min of treatment.

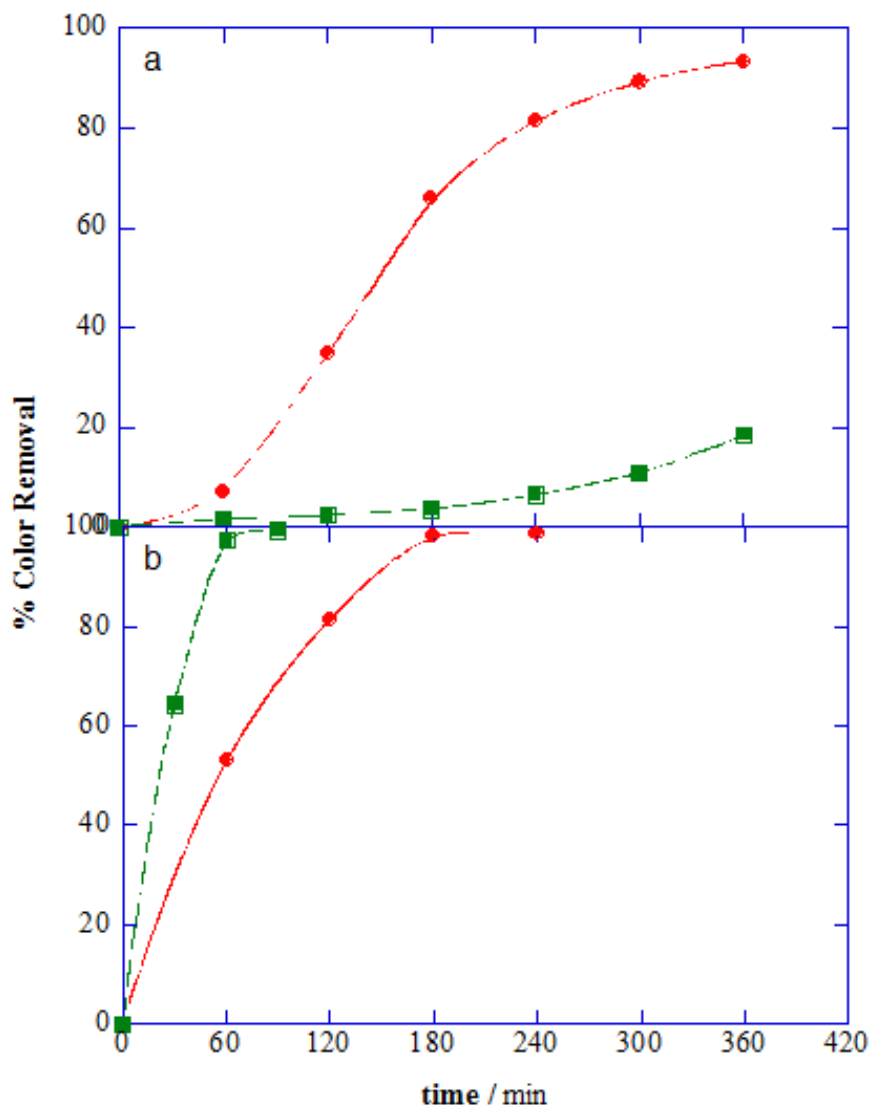


**Figure 3.** Removal color efficiency vs electrolysis time on the EO treatment of 1 L of 100 mg L<sup>-1</sup> MB at pH 6.0 and 25 °C at 60 mA cm<sup>-2</sup> using (●) Ti/Pt or (■) Ti/IrO<sub>2</sub>-Ta<sub>2</sub>O<sub>5</sub> anodes using (a) 0.05 mol L<sup>-1</sup> of Na<sub>2</sub>SO<sub>4</sub> or (b) 0.02 mol L<sup>-1</sup> Na<sub>2</sub>SO<sub>4</sub> and 0.017 mol L<sup>-1</sup> of NaCl as supporting electrolytes.

Conversely, when a low concentration of NaCl was added to the solution; a complete decolorization of solution was attained at both electrocatalytic materials. However, the elimination rate of the color depends on the anode material because at Ti/IrO<sub>2</sub>-Ta<sub>2</sub>O<sub>5</sub> anode, complete decolorization is attained at 60 min while that, Ti/Pt anode completed decolorization after 180 min of electrolysis. This trend is an indicative that the presence of chloride ion in solution plays a key role on the electrogeneration of different oxidant species [2,4,26]. In sulfate medium, the oxidation of water is the predominant reaction that yields reactive oxygen species such the adsorbed •OH according to reaction (1) [26]. However, when chloride is present in solution, active chlorine species are electrochemically produced and after, these are released into the bulk [27-29]. Later conditions strongly depend on the pH conditions, and consequently, under experimental conditions used here, Cl<sub>2</sub>, HClO and ClO<sup>-</sup> may be formed [7,30]. Thus, the homogeneous character of active chlorine species favors a rapid

elimination of color from solution at Ti/IrO<sub>2</sub>-Ta<sub>2</sub>O<sub>5</sub> anode because these species attack the chromophore group of dye while the  $\bullet$ OH radicals remain adsorbed onto the Ti/Pt surface, limiting the kinetic rate due to the dependence of the mass transfer of pollutants from solution towards the electrode [7,31]. Also, Cl<sub>2(g)</sub>-electrogeneration is preferentially favored at Ti/Pt, reducing the concentration of chlorine active species in solution, and consequently, decreasing its decolorization efficiency respect to Ti/IrO<sub>2</sub>-Ta<sub>2</sub>O<sub>5</sub> anode under similar experimental conditions. These figures are in agreement with the potentiodynamic measurements reported in Fig. 2.

### 3.2. Influence of the current density on decolorization

The applied current density ( $j$ ) is one of the major parameters of control of electrochemical processes that affects the electrokinetics and the extent of the reactions. Then,  $j$  controls the generation of M( $\bullet$ OH) by reaction (1) and the oxidation of Cl<sup>-</sup> and SO<sub>4</sub><sup>2-</sup> yielding the active chlorine species and persulfate by reactions (2-5) and (9), respectively in major or minor extent. As can be observed in Figure 4, an increase on the  $j$  using Na<sub>2</sub>SO<sub>4</sub> as supporting electrolyte accelerates the decolorization rate for both anodic materials. In the case of Ti/Pt, more than 88% of color removal is achieved at all  $j$  values after 300 min of electrolysis. Meanwhile, for Ti/IrO<sub>2</sub>-Ta<sub>2</sub>O<sub>5</sub> anode, no more than 20% of color removal was achieved. This trend evidences that, hydroxyl radicals are consumed when an increase on the  $j$  is attained, diminishing the overall decolorization efficiency and consequently, rising the energy consumption. These parasitic reactions involve primordially the oxidation of M( $\bullet$ OH) to O<sub>2</sub> at the anode by reaction (10), although it is also feasible its dimerization generating the less oxidant H<sub>2</sub>O<sub>2</sub> by reaction (11) or the direct O<sub>2</sub> evolution from water according to the oxygen evolution reaction (12) [3, 13].



On the other hand, the decolorization by homogeneous active chlorine species is faster than that with heterogeneous M( $\bullet$ OH), as discussed above. Nevertheless, the electrogeneration of active chlorine species seems to be limited by the applied  $j$ . A faster decolorization is achieved at Ti/Pt anode due to the combined action of M( $\bullet$ OH), persulfate and active chlorine species (Fig. 5a) when compared with the results reported in Fig. 4a. Although a noticeable enhancement on the decolorization kinetics is attained when Ti/IrO<sub>2</sub>-Ta<sub>2</sub>O<sub>5</sub> anode is used because short electrolysis times are spent independently of the applied  $j$  during EO of MB solution. This behavior is due to the efficient production of active chlorine species in solution, as discussed above. Besides, the use of high  $j$  is counterproductive since undesired hazardous chlorine species (chlorate and perchlorate) can be generated from parasitic reactions (13-15) [9,10,31]:





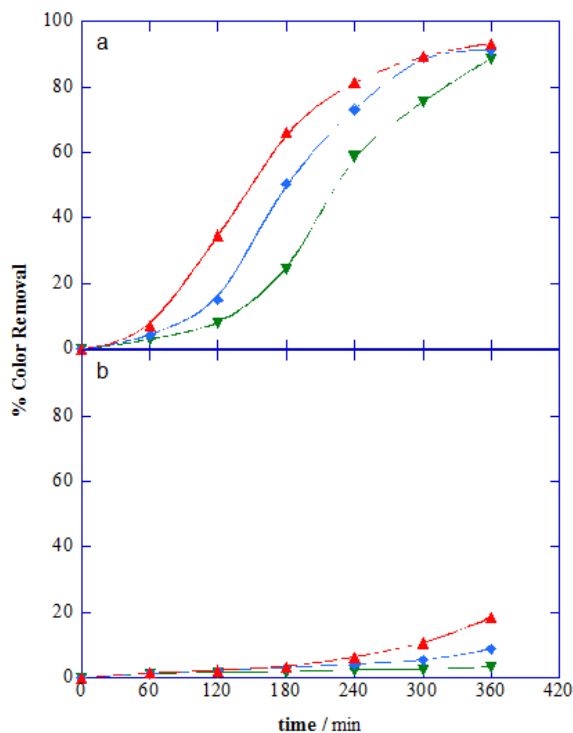


**Figure 4.** Percentage of color removal vs electrolytic time on the EO treatment of 1 L of 100 mg L<sup>-1</sup> MB with 0.05 mol L<sup>-1</sup> of Na<sub>2</sub>SO<sub>4</sub> at pH 6.0 and 25 °C using (a) Ti/Pt or (b) Ti/IrO<sub>2</sub>-Ta<sub>2</sub>O<sub>5</sub> anodes at applied current densities: (▼) 20, (◆) 40 and (▲) 60 mA cm<sup>-2</sup>.

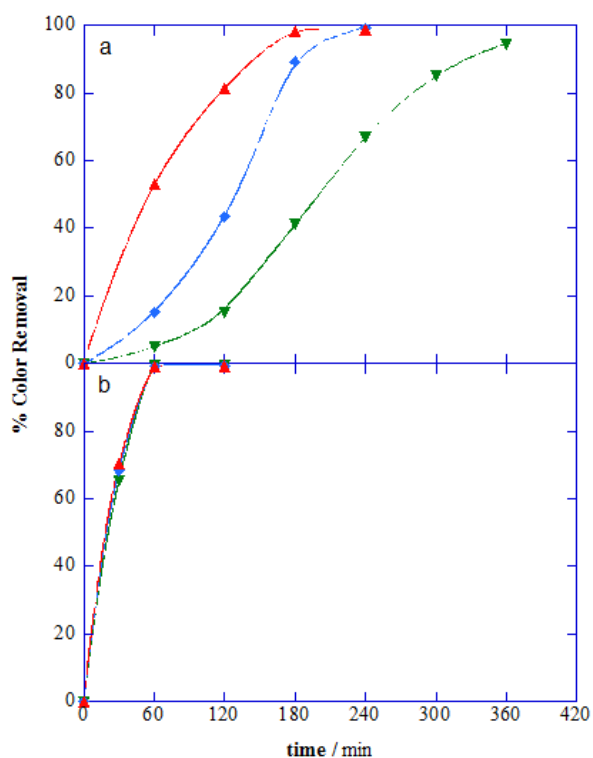


**Figure 5.** Percentage of color removal vs electrolytic time on the EO treatment of 1 L of 100 mg L<sup>-1</sup> MB with 0.02 mol L<sup>-1</sup> of Na<sub>2</sub>SO<sub>4</sub> and 0.017 mol L<sup>-1</sup> of NaCl at pH 6.0 and 25 °C using (a) Ti/Pt or (b) Ti/IrO<sub>2</sub>-Ta<sub>2</sub>O<sub>5</sub> anodes at applied  $j$ : (▼) 20, (◆) 40 and (▲) 60 mA cm<sup>-2</sup>.

### 3.3. Chemical oxygen demand abatement

The environmental regulation of several countries focuses mainly in the water effluent coloration, however the absence of coloration does not implies the removal of pollutants because some aromatic by-products could be uncolored. In this context, other parameters, such as COD, have significant relevance. The COD abatement is attained by the oxidation of the organic pollutants by the mediation of the oxidant species electrogenerated that conducts to their electrochemical incineration into  $\text{CO}_2$ , water and inorganic ions [1-4]. Figures 6a and b show the COD abatement after 360 min of EO treatment in absence and presence of chloride ion in the water matrix, respectively. Results clearly show that different degradation performances of MB solutions were achieved at both electrocatalytic materials using 0.05 M of  $\text{Na}_2\text{SO}_4$ . At  $\text{Ti}/\text{IrO}_2\text{-Ta}_2\text{O}_5$ , poor COD abatement was attained because of the oxygen evolution reaction is preferentially favored, as demonstrated by the polarization curves of Fig. 2b. It is mainly due to the amount of hydroxyl radicals electrogenerated from reaction (1). Also, these figures are consistent with the color removal (Fig. 4).

On the other hand, applied  $j$  plays a remarkable role on the organics mineralization [20,32] because an increase on the  $j$  from 40 to 60  $\text{mA cm}^{-2}$  promote a reduction on the COD abatement from 86.0 % down to 33.0 % (Fig. 6). This decay supposes a loss in % ICE when  $j$  increases. In fact, 9.36 % was estimated for 20  $\text{mA cm}^{-2}$ , 4.93 % for 40  $\text{mA cm}^{-2}$  and 1.26 % for 60  $\text{mA cm}^{-2}$ .

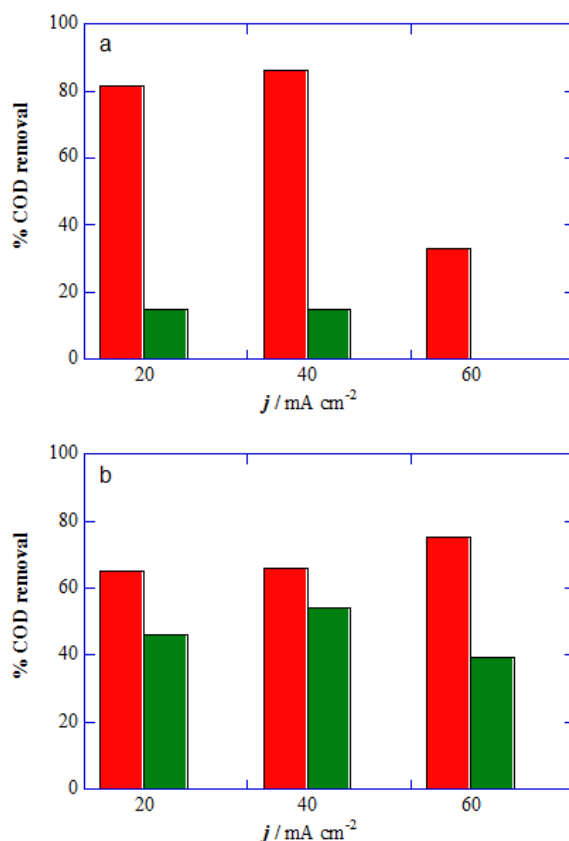


**Figure 6.** Percentage of chemical oxygen demand abatement attained after 360 min of EO treatment of 1 L of 100  $\text{mg L}^{-1}$  MB at pH 6.0 and 25 °C under different applied current densities using (■)  $\text{Ti}/\text{Pt}$  or (■)  $\text{Ti}/\text{IrO}_2\text{-Ta}_2\text{O}_5$  anodes in (a) 0.05  $\text{mol L}^{-1}$  of  $\text{Na}_2\text{SO}_4$  or (b) 0.02  $\text{mol L}^{-1}$   $\text{Na}_2\text{SO}_4$  and 0.017  $\text{mol L}^{-1}$  of  $\text{NaCl}$  as supporting electrolytes.

The loss in ICE is related to the enhancement of the parasitic reactions (10-11) and the oxygen evolution reaction (12) that reduces the  $M(\bullet\text{OH})$  generation and the number of organic events that conducts to mineralization.

Figure 6b evidences that the oxidative power of EO increases by using  $\text{Ti}/\text{IrO}_2\text{-Ta}_2\text{O}_5$  anode due to the electrogeneration of chlorine active species from chloride oxidation by reactions (2-5). Results clearly demonstrated that 54.5 % of COD abatement was achieved at  $40 \text{ mA cm}^{-2}$ , being much more superior to 15.0 % of COD removal under the same experimental conditions in absence of chloride. From these results we can conclude that chlorine active species apart from enhancing the decolorization rate also contribute to the oxidization of organics [2,31,34]. However, it is important to notice that  $\text{Ti}/\text{Pt}$  achieved a decrease of ca. 20 % of COD abatement in the presence of chloride. This result can be explained by the lower electrogeneration of  $M(\bullet\text{OH})$  due to the competitive reactions of electrochlorination. Nonetheless, the coexistence of a feasible side-effect of chlorine active species can be attained by the generation of organochlorinated compounds. Then, these species are usually more recalcitrant and hardly oxidizable than non-chlorinated derivatives [7,9], reducing the mineralization efficiency. Besides, the formation of chlorinated derivatives must avoided due to their high toxicity and suspicious carcinogenicity [9,10,35].

### 3.4. Estimation of Energy Consumption

The operation energy requirement is directly related to the operational conditions such as the applied  $j$ , the nature of the electrodic material and the supporting electrolyte. Consequently, the optimum parameter conditions must be related not only with the decolorization rate or the percentage of COD removal but also with energy consumption (EC), which further defines the operational costs. Thus, the EC in  $\text{kWh m}^{-3}$  of the process per volume of treated wastewater was determined from equation (16) [23,26]:

$$EC = \frac{\Delta E_c It}{1000 V_s} \quad (16)$$

where,  $\Delta E_c$  is the average cell voltage in V and  $V_s$  the volume treated in  $\text{m}^3$ .

Table 2 summarizes the EC estimated by Eq. (16) and the process expenditure in order to assess the economic feasibility of EO as a green sustainable alternative for dyestuff effluents. The cost was determined taking into consideration the electrical energy cost of about R\$ 0.32 (Brazilian price, taxes excluded) per kWh (Agência Nacional de Energia Elétrica, Brazil). This price was also included in dollar currency. EC requirements and costs are both proportional to the applied  $j$ , for example, 4.82 US\$  $\text{m}^{-3}$  up to 39.18 US\$  $\text{m}^{-3}$  were estimated when  $j$  passed from 20 up to  $60 \text{ mA cm}^{-2}$ .

Although the costs associated could appear higher than those associated to conventional water treatment technologies, the higher effectivity of EO to recover the hydric resources and to improve the average quality of water effluents is undoubtedly a factor of major relevance than the economic aspect. Apart from that, the possible implementation of renewable energy sources could cut down to zero the associated cost of EO by the in situ production of the required energy using solar panels[36,37] or wind mills [38].

**Table 2.** Estimated energy consumption and operational cost for the EO treatment of MB solutions at the pre-pilot flow plant.

Experimental conditions			Energy consumption (kWh m <sup>-3</sup> )	Cost (US\$ m <sup>-3</sup> )
Anode	Electrolyte	j (mA cm <sup>-2</sup> )		
Ti/IrO <sub>2</sub> -Ta <sub>2</sub> O <sub>5</sub>	0.05 M Na <sub>2</sub> SO <sub>4</sub>	20.0	57.9	4.82
		40.0	175.3	14.58
		60.0	326.9	27.20
	0.05 M Na <sub>2</sub> SO <sub>4</sub> and 0.017 M NaCl	20.0	93.0	7.74
		40.0	256.0	21.30
		60.0	475.5	39.56
Ti/Pt	0.05 M Na <sub>2</sub> SO <sub>4</sub>	20.0	65.5	5.45
		40.0	196.6	13.36
		60.0	358.9	29.94
	0.05 M Na <sub>2</sub> SO <sub>4</sub> and 0.017 M NaCl	20.0	80.8	6.72
		40.0	237.7	19.78
		60.0	470.9	39.18

Thus, taking into account all the results reported here, the use of Ti/Pt anode in EO in 0.05 M Na<sub>2</sub>SO<sub>4</sub> at 40 mA cm<sup>-2</sup> could be considered the optimal EO treatment conditions that allow obtaining higher COD abatement and total decolorization with the lower cost associated.

#### 4. CONCLUSIONS

EO is a highly promising electrochemical technology to remediate the water pollution and reduce the environmental impact of human activity. The process has been scaled-up using an electrochemical filter-press cell reactor to evaluate the decolorization and mineralization of MB solutions. In addition the treatment performance has been evaluated depending on the anodic material, supporting electrolyte and the applied current density. It has been found that the presence of chloride ion in solution promotes the electrogeneration of active chlorine species as oxidant mediators. Although the decolorization is appreciably accelerated by the presence of active chlorine species, the COD abatement obtained at the end of the treatment was lower than the EO using Na<sub>2</sub>SO<sub>4</sub> as supporting electrolyte. The applied current density has been also studied as key parameter in electrochemistry being defined 40 mA cm<sup>-2</sup> as the optimal operational condition to reach satisfactorily the maximum DOC abatement of 86.0 % and complete decolorization using Ti/Pt anodes. Affordable costs of process expenditure of 13.36 US\$ m<sup>-3</sup> have been estimated using Ti/Pt anodes under optimal conditions after 6h of treatment; however, these costs could be reduced increasing the solution conductivity. These promising results encourage the development of further EO studies at pre-pilot plant scale with other anodic materials to treat actual effluents.

## ACKNOWLEDGEMENTS

Brazilian financial support from National Council for Scientific and Technological Development (CNPq - 446846/2014-7 and CNPq - 401519/2014-7) is gratefully acknowledged. J.P.S.D. Pontes and P.R.F. da Costa acknowledge the PhD grants awarded from CNPq. S. Garcia-Segura gratefully acknowledges the post-doctoral fellowship awarded from and PNPd/CAPES.

## References

1. M. Panizza, G. Cerisola, *Chem. Rev.* 109 (2009) 6541-6569.
2. C.A. Martínez-Huitle, M.A. Rodrigo, I. Sirés, O. Scialdone, *Chem. Rev.* 115 (2015) 13362-13407.
3. E. Brillas, I. Sirés, M.A. Oturan, *Chem. Rev.* 109 (2009) 6570-6631.
4. C.A. Martínez-Huitle, S. Ferro, *Chem. Soc. Rev.* 35 (2006) 1324-1340.
5. Q. Dai, Y. Xia, L. Jiang, W. Li, J. Wang, J. Chen, *Int. J. Electrochem. Sci.* 7 (2012) 12895-12906.
6. N. Contreras, J. Vidal, C. Berrios, L. Villegas, R. Salazar, *Int. J. Electrochem. Sci.* 10 (2015) 9269-9285.
7. S. Garcia-Segura, J. Keller, E. Brillas, J. Radjenovic, *J. Hazard. Mater.* 283 (2015) 551-557.
8. D. Rajkumar, B.J. Song, J.G. Kim, *Dyes Pigments* 72 (2007) 1-7.
9. J. Radjenovic, D.L. Sedlak, *Environ. Sci. Technol.* 49 (2015) 11292-11302.
10. M.E.H. Bergmann, J. Rollin, T. Iourtchouk, *Electrochim. Acta* 54 (2009) 2102-2107.
11. E. do Vale-Júnior, S. Dosta, I.G. Cano, J.M. Guilemany, S. Garcia-Segura, C.A. Martínez-Huitle, *Chemosphere* 148 (2016) 47-54.
12. E. Brillas, C.A. Martínez-Huitle, *Appl. Catal. B: Environ.* 166-167 (2015) 603-643.
13. X. Florenza, A.M.S. Solano, F. Centellas, C.A. Martínez-Huitle, E. Brillas, S. Garcia-Segura, *Electrochim. Acta* 142 (2014) 276-288.
14. H.S. Freeman, E. Jeong, L.D. Claxton, *Dyes Pigments* 99 (2013) 496-501.
15. A.C. Couto, J.D. Ferreira, A.C.S. Rosa, M.S. Pombo-de-Oliveira, S. Koifman, *Chem-Biol. Interact.* 205 (2013) 46-52.
16. C. Wang, F. Wang, M. Xu, C. Zhu, W. Fang, Y. Wei, *J. Electroanal. Chem.* 759 (2015) 158-166.
17. S. Janani, K.S.S. Rani, P. Ellappan, L.R. Miranda, *J. Environ. Chem. Eng.* 4 (2016) 534-541.
18. M.B. Ferreira, J.H.B. Rocha, J.V. Melo, C.A. Martínez-Huitle, M.A.Q. Alfaro, *Electrocatalysis* 4 (2013) 274-282.
19. Y. He, E. Dong, W. Huang, X. Tang, H. Liu, H. Lin, H. Li, *J. Electroanal. Chem.* 759 (2015) 167-173.
20. V.S. Antonin, M.C. Santos, S. Garcia-Segura, E. Brillas, *Water Res.* 83 (2015) 31-41.
21. H. Olvera-Vargas, N. Oturan, E. Brillas, D. Buisson, G. Esposito, M. Oturan, *Chemosphere* 117 (2014) 644-651.
22. H.T. Madsen, E.G. Søgaard, J. Muff, *Chemosphere* 120 (2015) 756-763.
23. S. Garcia-Segura, L.C. Almeida, N. Bocchi, E. Brillas, *J. Hazard. Mater.* 194 (2011) 109-118.
24. F.L. Souza, C. Saéz, M.R.V. Lanza, P. Cañizares, M.A. Rodrigo, *Appl. Catal. B: Environ.* 180 (2016) 733-739.
25. C. Salazar, I. Sirés, R. Salazar, H.D. Mansilla, C.A. Zaror, *J. Chem. Technol. Biotechnol.* 90 (2015) 2017-2026.
26. P.R.F. da Costa, D.R. da Silva, C.A. Martínez-Huitle, S. Garcia-Segura, *J. Electroanal. Chem.* 763 (2016) 97-103.
27. J. Wu, Z. He, X. Du, C. Zhang, D. Fu, *J. Taiwan Inst. Chem. Eng.* 59 (2016) 303-310.
28. A. Uranga-Flores, C. de la Rosa-Júarez, S. Gutierrez-Granados, D.C. de Moura, C.A. Martínez-Huitle, J.M. Peralta-Hernández, *J. Electroanal. Chem.* 738 (2015) 84-91.
29. A. Thiam, E. Brillas, F. Centellas, P.L. Cabot, I. Sirés, *Electrochim. Acta* 173 (2015) 523-533.
30. M. Deborde, U. von Gunten, *Water Res.* 42 (2008) 13-51.

31. C.N. Brito, D.R. da Silva, S. Garcia-Segura, D.C. de Moura, C.A. Martínez-Huitile, *J. Electrochem. Soc.* 163 (2016) E62-E69.
32. F. L. Guzmán-Duque, R.E. Palma-Goyes, I. González, G. Peñuela, R.A. Torres-Palma, *J. Hazard. Mater.* 278 (2014) 221-226.
33. G.K. Chandler, J.D. Genders, D. Pletcher, *Platin. Met. Rev.* 41 (1997) 54-63.
34. O. Scialdone, S. Randazzo, A. Galia, G. Silvestri, *Water Res.* 43 (2009) 2260-2272.
35. R. Menzies, N.S. Quinete, P. Gardinali, D. Seba, *Mar. Pollut. Bull.* 70 (2013) 289–295.
36. S. Garcia-Segura, E. Brillas, *Electrochim. Acta* 140 (2014) 384-395.
37. S. Garcia-Segura, E. Brillas, *Appl. Catal. B: Environ.* 181 (2016) 681-691.
38. F.L. Souza, M.R.V. Lanza, J. Llanos, C. Sáez, M.A. Rodrigo, P. Cañizares, *J. Environ. Manage.* 158 (2015) 36-39.

© 2016 The Authors. Published by ESG ([www.electrochemsci.org](http://www.electrochemsci.org)). This article is an open access article distributed under the terms and conditions of the Creative Commons Attribution license (<http://creativecommons.org/licenses/by/4.0/>).